Cite as: Wang X, Tian D, Du M. Application of ultrasound combined with contrast-enhanced ultrasound in the diagnosis of axillary lymph node metastasis of breast cancer [J]. Chin J Clin Res, 2026, 39(4): 533-537,542.

DOI: 10.13429/j.cnki.cjcr.2026.04.009

Application of ultrasound combined with contrast-enhanced ultrasound in the diagnosis of axillary lymph node metastasis of breast cancer

WANG Xin*, TIAN Dan, DU Min

* *Department of Ultrasonography, Inner Mongolia Hospital Beijing Hospital of Traditional Chinese Medicine, Bayannur, Inner Mongolia 015000, China*

Corresponding author: WANG Xin, E-mail: 18547828505@163.com

Abstract: **Objective** To analyze the diagnostic value of ultrasound (US) combined with contrast-enhanced ultrasound (CEUS) in axillary lymph node metastasis of breast cancer, and to identify the related independent risk factors. **Methods** A retrospective selection was made of 102 breast cancer patients admitted to Inner Mongolia Hospital Beijing Hospital of Traditional Chinese Medicine from January 2022 to December 2024. All patients completed US, CEUS, magnetic resonance imaging (MRI) , and mammography examinations in sequence within one week before surgery, with non - simultaneous one -time operations, and the examinations were conducted at different time periods in accordance with clinical diagnosis and treatment norms. Patients were diagnosed by histopathological examination. The postoperative lymph node pathological results were used as the gold standard, and Kappa value was used to evaluate the diagnostic consistency of each examination. Receiver operating characteristic (ROC) curve was used to evaluate itsdiagnostic value, and multivariate logistic regression was used to screen independent risk factors (stepwise regression method was used to control the number of variables). **Results** Among 102 patients, 37 cases (36.27%) were pathologically diagnosed with lymph node metastasis. The Kappa value of US combined with CEUS was 0.936, the accuracy was 0.971, the specificity was 0.985, and the sensitivity was 0.946. ROC curve showed that the area under the curve (AUC) of combined examination was 0.965(95%*CI*: 0.919-1.000) , which was significantly higher than that of single US(AUC=0.811, 95%*CI*: 0.715-0.907), CEUS(AUC=0.882, 95%*CI*: 0.802-0.963) , MRI (AUC=0.853, 95%*CI*: 0.766- 0.941) , and mammography (AUC=0.803, 95% *CI*: 0.707- 0.900) (P<0.05). Multivariate logistic regression analysis showed that in US and CEUS imaging, tumor diameter ≥2 cm, maximum cortical thickness of lymph nodes ≥3 mm, and irregular enhancement pattern were independent risk factors for axillary lymph node metastasis of breast cancer (P<0.05) . **Conclusion** The combined examination of US and CEUS has high application value in the diagnosis of axillary lymph node metastasis of breast cancer, and the diagnostic efficacy is better than single US, CEUS, traditional MRI and mammography, which can provide reliable basis for clinical diagnosis and treatment.

Keywords: Ultrasound; Contrast-enhanced ultrasound; Breast cancer; Axillary lymph node metastasis; Pathology; Tumor diameter; Cortical thickness of lymph mode

Fund program: Youth Fund Project of Natural Science Foundation of Inner Mongolia Autonomous Region(2023QN08044)

Lymph node metastasis is one of the common metastatic pathways of breast cancer and a key factor affecting prognosis. Once cancer cells spread to axillary lymph nodes through lymphatic vessels, the difficulty of clinical treatment increases significantly[1-2]. Studies have shown that the 5-year survival rate of breast cancer patients with axillary lymph node metastasis is significantly lower than that of patients without metastasis, and the number and location of metastatic lymph nodes are closely related to patients' recurrence risk and survival time[3]. At present, ultrasound is one of the methods for breast cancer screening and diagnosis, which can clearly show the morphology and structure of breast and axillary lymph nodes, and can observe the aspect ratio, blood flow signal and other characteristics of lymph nodes[4-5]. However, its diagnostic accuracy for tiny or atypical metastatic lymph nodes is limited. Contrast-enhanced ultrasound can clearly display the internal structure and blood flow distribution of lymph nodes, and has high sensitivity and specificity for the diagnosis of lymph node metastasis[6], but it is subjective and has high technical requirements. This study combines ultrasound and contrast-enhanced ultrasound to give full play to their advantages, improve the diagnostic accuracy of breast cancer axillary lymph node metastasis, and clarify relevant risk factors, so as to provide a better clinical diagnosis scheme.

1 Materials and Methods

1.1 General Information

A total of 102 breast cancer patients admitted to Inner Mongolia Hospital of Beijing Hospital of Traditional Chinese Medicine from January 2022 to December 2024 were retrospectively selected, aged 30-81 (56.27±10.61) years. Pathological types: 82 cases of invasive ductal carcinoma, 12 cases of invasive lobular carcinoma, 5 cases of mucinous adenocarcinoma, and 3 cases of other types. All patients signed informed consent, and this study was approved by the Medical Ethics Committee of Inner Mongolia Hospital of Beijing Hospital of Traditional Chinese Medicine (Ethics Approval No.: BIZ20211207).

1.2 Inclusion and Exclusion Criteria

(1) **Inclusion criteria**: ① All patients met the diagnostic criteria for breast cancer[7] and were confirmed by histopathological examination; ② Age ≥ 18 years old; ③ All were female; ④ First onset of unilateral disease; ⑤ No anti-tumor treatment was received before surgery, and complete preoperative imaging evaluation could be completed. (2) **Exclusion criteria**: ① Complicated with other malignant tumors; ② Allergic to ultrasound contrast agents; ③ Severe dysfunction of important organs such as heart, liver and kidney; ④ History of mental illness or cognitive impairment; ⑤ Have received neoadjuvant chemotherapy, radiotherapy or endocrine therapy, etc.

1.3 Instruments and Equipment

LOGIQ Fortis ultrasonic diagnostic instrument (GE Healthcare Medical Systems (China) Co., Ltd.), EPIQ7 color ultrasonic diagnostic system (Philips Ultrasound Co., Ltd.), 3.0T magnetic resonance imaging system (Siemens Healthineers), and digital mammography system (Hologic Medical Technology Co., Ltd.) were used in this study.

1.4 Methods

All imaging data were independently analyzed by two experienced physicians, and a consensus was reached through negotiation when opinions were inconsistent. All imaging examinations were completed on separate days within 1 week before surgery in the order of ultrasound → contrast-enhanced ultrasound → mammography → magnetic resonance imaging (MRI), so as to avoid patient discomfort and image interference caused by excessive single examinations.

1.4.1 Ultrasound

The ultrasonic diagnostic instrument equipped with a high-frequency linear array probe with a frequency of 4-13 MHz was used. During ultrasound examination, patients were required to fully expose their chest and take the supine position, supplemented by the lateral position if necessary. Two-dimensional ultrasound was used to conduct comprehensive and meticulous multi-section scanning of bilateral breasts and axillae. The hierarchical structure of the breast, as well as the location, size, shape, boundary, internal echo and posterior echo of the mass were carefully observed. The color Doppler ultrasound function was activated to detect the blood flow of breast masses and axillary lymph nodes. The distribution of blood flow signals inside and around the mass was observed, and the richness of blood flow, vascular course and blood flow spectrum characteristics were recorded. Typical cases are shown in **Figure 1**.

1.4.2 Contrast-Enhanced Ultrasound

The examination was performed on the basis of conventional ultrasound. 5 mL of ultrasound contrast agent (Sulfur Hexafluoride Microspheres for Injection, trade name: SonoVue, manufacturer: Bracco Suisse SA, batch number: F241008Z, diluted and shaken with 5 mL of normal saline) was rapidly injected as a bolus via the elbow vein, followed immediately by a rapid flush with 10 mL of normal saline. At the same time of contrast agent injection, the contrast imaging mode of the ultrasonic diagnostic instrument was activated to dynamically observe the contrast agent perfusion of breast masses and axillary lymph nodes in real time. The observation lasted for 3 minutes, and the onset time of contrast agent enhancement, enhancement mode, enhancement intensity, time to peak, clearance rate and other parameters were recorded in detail. Typical cases are shown in **Figure 2**.

1.4.3 Mammography

Patients took the standing position, and craniocaudal view and mediolateral oblique view of bilateral breasts were taken, and lateral view was added if necessary. Photography parameters: tube voltage 26-32 kV, tube current 60-80 mA, exposure time 0.15-0.35 s, automatic exposure control mode, which met the quality control standards for mammography.

1.4.4 MRI

Patients took the prone position with a dedicated breast coil, and axial T1-weighted imaging (T1WI), T2-weighted imaging (T2WI) and dynamic contrast-enhanced scanning were performed. Scanning parameters: repetition time 500 ms and echo time 10 ms for T1WI; repetition time 3 000 ms and echo time 80 ms for T2WI. Gadopentetate dimeglumine was used as the contrast agent for dynamic contrast-enhanced scanning at a dose of 0.1 mmol/kg, which was injected as a bolus via the elbow vein followed by immediate scanning for 5 consecutive phases, with each phase lasting 30 s.

1.5 Diagnostic Criteria for Lymph Node Metastasis

The results of postoperative pathological examination of lymph nodes were taken as the gold standard. The diagnostic criteria for ultrasound and contrast-enhanced ultrasound were as follows: (1) lymph node enlargement, with an aspect ratio < 2, even close to 1; (2) blurred boundary and uneven internal echo; (3) cortical thickening > 3 mm; (4) destruction, displacement or disappearance of the lymph hilum; (5) abundant and irregularly distributed blood flow signals, manifested as peripheral blood flow or mixed blood flow; (6) microcalcification in lymph nodes[8]. Patients were divided into the metastatic group and the non-metastatic group according to the presence of lymph node metastasis.

1.6 Statistical Methods

SPSS 26.0 software was used for data analysis. Measurement data conforming to normal distribution were expressed as $\bar{x}\pm s$, and t-test was used. Count data were expressed as cases (%), and the χ^2 test or corrected χ^2 test was used. The Kappa value was used to evaluate the consistency of different examinations in the diagnosis of axillary lymph node metastasis of breast cancer. The receiver operating characteristic (ROC) curve was used to evaluate the value of combined examination in the diagnosis of axillary lymph node metastasis of breast cancer. The stepwise method (entry significance level α_{in}=0.05, removal significance level α_{out}=0.10) was used for multivariate logistic regression, and the number of independent variables was controlled (3 variables were finally included). The sample size was estimated based on the metastasis rate (30%) in previous studies, with α=0.05 and β=0.20, and the calculated minimum sample size was 92 cases, which was satisfied by the 102 cases included in this study. A P value < 0.05 was considered statistically significant.

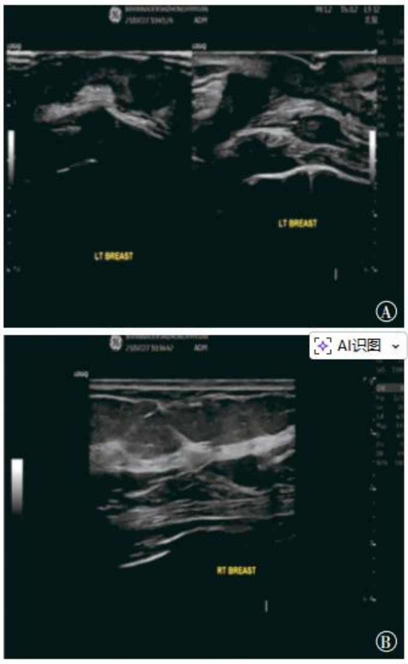

Note: A, After left breast resection, heterogeneous hypoechoic lesions were observed along the incision course, with clear boundaries and irregular morphology. Color Doppler Flow Imaging (CDFI) showed a small amount of local blood flow signals. Multiple similar hypoechoic lesions were seen deep to the medial incision, with the largest one measuring 0.78 cm × 0.90 cm, which had unclear boundaries, irregular morphology and infiltrative features. **B,** The glandular lobe structure of the right breast was clear, the parenchymal echo was uniform, and no specific space-occupying lesion was found. No obvious abnormal enlarged lymph nodes were observed in bilateral axillae. Multiple solid masses at the left breast incision scar and deep to the scar.

Fig.1 Ultrasound examination images of typical cases

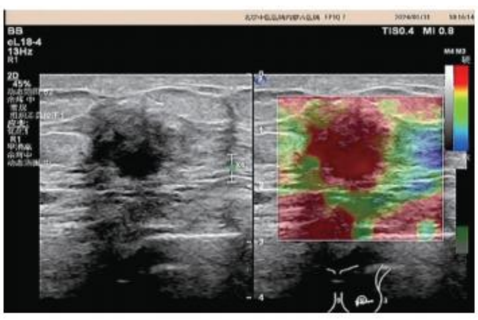

Note: The glandular lobe structure of the breast is clear. A 1.58 cm × 1.43 cm hypoechoic lesion is observed adjacent to the nipple at the 5 o'clock position of the left breast, with irregular morphology, unclear boundary and heterogeneous echo. Color Doppler Flow Imaging shows a small amount of blood flow signals in the periphery and inside of the lesion. Solid nodule in the left breast, BI-RADS category 4b.

Fig.2 Contrast-enhanced ultrasound images of typical cases

2 Results

2.1 Diagnostic Consistency and Diagnostic Efficacy

Among the 102 patients, 37 (36.27%) had lymph node metastasis. Taking pathological results as the gold standard, the Kappa value of ultrasound was 0.633, with an accuracy of 0.833, a specificity of 0.892, a sensitivity of 0.730, a positive predictive value of 0.794, and a negative predictive value of 0.853. The Kappa value of contrast-enhanced ultrasound was 0.783, with an accuracy of 0.902, a specificity of 0.954, a sensitivity of 0.811, a positive predictive value of 0.909, and a negative predictive value of 0.899. The Kappa value of MRI was 0.719, with an accuracy of 0.872, a specificity of 0.923, a sensitivity of 0.784, a positive predictive value of 0.853, and a negative predictive value of 0.882. The Kappa value of mammography was 0.614, with an accuracy of 0.824, a specificity of 0.877, a sensitivity of 0.730, a positive predictive value of 0.771, and a negative predictive value of 0.851. The Kappa value of the combined examination of ultrasound and contrast-enhanced ultrasound was 0.936, with an accuracy of 0.971, a specificity of 0.985, a sensitivity of 0.946, a positive predictive value of 0.972, and a negative predictive value of 0.970. It can be seen that the combined examination has better diagnostic consistency and higher diagnostic efficacy, as shown in **Table 1**.

Tab.1 Consistency in lymph node metastasis diagnosis (n=102, case)

Item		Pathological result		Total
		Positive (n=37)	Negative (n=65)	
Ultrasound	Positive	27	7	34
	Negative	10	58	68
Contrast-enhanced ultrasound	Positive	30	3	33
	Negative	7	62	69
MRI	Positive	29	5	34
	Negative	8	60	68
Mammography	Positive	27	8	35
	Negative	10	57	67
Combined ultrasound and contrast-enhanced ultrasound	Positive	35	1	36
	Negative	2	64	66
Total		37	65	102

2.2 Diagnostic Value of Different Examinations

The ROC curve showed that the area under the curve (AUC) of the combined examination was significantly higher than that of single ultrasound, contrast-enhanced ultrasound, MRI, and mammography (P < 0.05), as shown in **Figure 3** and **Table 2**.

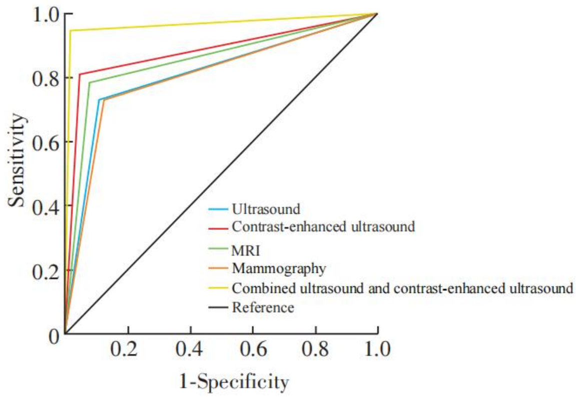

Fig.3 ROC curves of different examinations for the diagnosis of axillary lymph node metastasis in breast cancer

Tab.2 Diagnostic value of different examinations for axillary lymph node metastasis in breast cancer

Item	AUC	*SE*	*P* value	95%*CI*
Ultrasound	0.811	0.049	<0.001	0.715-0.907
Contrast-enhanced ultrasound	0.882	0.041	<0.001	0.802-0.963
MRI	0.853	0.044	<0.001	0.766-0.941
Mammography	0.803	0.049	<0.001	0.707-0.900
Combined ultrasound and contrast-enhanced ultrasound	0.965	0.023	<0.001	0.919-1.000

2.3 Comparison of Clinical Data Between the Metastatic Group and the Non-Metastatic Group

There were no statistically significant differences in age, body mass index (BMI), menopause status, hypertension, diabetes, pathological type, tumor location and other data between the metastatic group and the non-metastatic group (P > 0.05), while the difference in TNM staging was statistically significant (P < 0.05), as shown in **Table 3**.

2.4 Comparison of Imaging Features Between the Metastatic Group and the Non-Metastatic Group

There were no statistically significant differences in vascular invasion, uneven internal echo, posterior echo attenuation, irregular shape, calcification, spiculated margin, aspect ratio, blood flow grade, maximum longitudinal diameter of lymph nodes, enhancement degree, structural distortion, clear boundary after enhancement, enlarged range after enhancement, perfusion defect after enhancement, and radial convergence at the margin after enhancement between the metastatic group and the non-metastatic group (P > 0.05). There were statistically significant differences in tumor diameter, maximum cortical thickness of lymph nodes, and irregular enhancement mode between the two groups (P < 0.05), as shown in **Table 4**.

Tab.3 Comparison of clinical data between metastatic group and non-metastatic group [case(%)]

Item	Metastatic group（n=37）	Non-metastatic group（n=65）	t/χ^2 value	*P* value
Age（years, $\bar{x}\pm s$）	55.59±10.81	56.66±10.55	0.488	0.626
BMI（kg/m², $\bar{x}\pm s$）	22.16±1.42	22.51±1.53	1.140	0.257
Menopause [cases (%)]	14（37.84）	35（53.85）	2.421	0.120
Hypertension [cases (%)]	13（35.14）	24（36.92）	0.033	0.857
Diabetes mellitus [cases (%)]	10（27.03）	15（23.08）	0.199	0.656
TNM stage [cases (%)]			32.464	<0.001
Stage I-II	15（40.54）	60（92.31）		
Stage III-IV	22（59.46）	5（7.69）		
Pathological type [cases (%)]			0.090	0.993
Invasive ductal carcinoma	30（81.08）	52（80.00）		
Invasive lobular carcinoma	4（10.81）	8（12.31）		
Mucinous adenocarcinoma	2（5.41）	3（4.62）		
Other types	1（2.70）	2（3.07）		
Tumor side [cases (%)]			0.395	0.530
Left side	16（43.24）	24（36.92）		
Right side	21（56.76）	41（63.08）		

Tab.4 Comparison of imaging features between the metastatic group and the non-metastatic group [case (%)]

Item	Metastatic group（n=37）	Non-metastatic group（n=65）	χ^2 value	*P* value
Vascular invasion	22（59.46）	36（55.38）	0.160	0.690
Heterogeneous internal echo	25（67.57）	32（49.23）	3.216	0.073
Posterior echo attenuation	11（29.73）	16（24.62）	0.317	0.573
Irregular shape	26（70.27）	42（64.62）	0.339	0.560
Calcification	15（40.54）	22（33.85）	0.457	0.499
Spiculated margin	17（45.95）	40（61.54）	2.325	0.127
Tumor diameter			30.404	<0.001
<2 cm	9（24.32）	52（80.00）		
≥2 cm	28（75.68）	13（20.00）		
Aspect ratio			1.308	0.253
<1	15（40.54）	34（52.31）		

≥1	22（59.46）	31（47.69）		
Blood flow grade			3.435	0.064
Grade I-II	14（37.84）	37（56.92）		
Grade III	23（62.16）	28（43.08）		
Maximum longitudinal diameter of lymph node			2.968	0.085
<1 cm	26（70.27）	55（84.62）		
≥1 cm	11（29.73）	10（15.38）		
Maximum cortical thickness of lymph node			29.397	<0.001
<3 mm	8（21.62）	50（76.92）		
≥3 mm	29（78.38）	15（23.08）		
Enhancement degree			0.012	0.912
Hypoenhancement/Isoenhancement	6（16.22）	10（15.38）		
Hyperenhancement	31（83.78）	55（84.62）		
Structural distortion	7（18.92）	4（6.15）	2.777	0.096
Irregular enhancement pattern	30（81.08）	26（40.00）	16.071	<0.001
Clear boundary after enhancement	9（24.32）	19（29.32）	0.285	0.593
Enlarged range after enhancement	30（81.08）	42（64.62）	3.079	0.079
Perfusion defect after enhancement	12（32.43）	17（26.15）	0.457	0.499
Radial convergence at margin after enhancement	11（29.73）	15（23.08）	0.549	0.459

Tab.5 Multivariate logistic regression analysis of axillary lymph node metastasis in breast cancer

Index	β	*SE*	Wald χ^2	*OR* value	95% *CI*	*P* value
Tumor diameter ≥2 cm	1.286	0.626	4.222	3.619	1.061-12.343	0.040
Maximum cortical thickness of lymph node ≥3 mm	1.277	0.629	4.120	3.587	1.045-12.314	0.042
Irregular enhancement pattern	1.217	0.609	3.993	3.377	1.024-11.139	0.046

3 Discussion

This study focused on the diagnostic value of combined ultrasound and contrast-enhanced ultrasound for axillary lymph node metastasis in breast cancer, and clarified its clinical application advantages through direct comparison with MRI and mammography. In terms of diagnostic consistency, the Kappa value of the combined examination for consistency with pathological results was as high as 0.936, which was much higher than that of single ultrasound (0.633), contrast-enhanced ultrasound (0.783), MRI (0.719) and mammography (0.614), indicating that the combined examination has an extremely high degree of agreement with the pathological gold standard, and the diagnostic results are more reliable. In terms of diagnostic efficacy, the accuracy (0.971), specificity (0.985) and sensitivity (0.946) of the combined examination were significantly better than those of single examination methods. The essence of this advantage is the complementary synergy of the two technologies: ultrasound can clearly present the morphological characteristics of lymph nodes (such as size, boundary, cortical thickness, etc.), providing a structural basis for preliminary judgment[9]; while contrast-enhanced ultrasound can accurately display the blood flow perfusion pattern. Metastatic lymph nodes often show characteristics such as irregular enhancement and perfusion defects, which can effectively distinguish reactive hyperplastic lymph nodes with similar morphology. Although MRI has high soft tissue resolution, it is greatly interfered by respiratory motion, has limited detection rate for tiny metastatic foci, and has high examination cost and long time consumption, which is not conducive to promotion in primary medical institutions[10]. Mammography is sensitive to calcification foci, but has insufficient penetration into dense breast tissue and poor display effect on axillary lymph nodes[11], resulting in a sensitivity of only 0.730, which is lower than that of the combined examination. ROC curve analysis further confirmed that the AUC of the combined examination (0.965) was significantly higher than that of MRI (0.853) and mammography (0.803), indicating that its diagnostic accuracy is higher, and it can more effectively identify whether axillary lymph nodes are metastasized, providing a key basis for the formulation of clinical treatment plans.

Through multivariate logistic regression analysis, this study clarified that tumor diameter ≥ 2 cm, maximum cortical thickness of lymph nodes ≥ 3 mm, and irregular enhancement pattern in ultrasound and contrast-enhanced ultrasound images were independent risk factors for axillary lymph node metastasis in breast cancer. The larger the tumor diameter, the higher the probability that cancer cells break through the basement membrane and invade the lymphatic vessels, and the risk of lymph node metastasis increases accordingly[12]. The maximum cortical thickness of lymph nodes ≥ 3 mm reflects the abnormal proliferation of lymph node structure, which is a direct manifestation of metastatic foci invasion[13]. The irregular enhancement pattern indicates disordered blood flow perfusion inside the lymph nodes, which is closely related to the invasive biological behavior of metastatic lesions[14]. The clarification of these risk factors helps clinicians focus on relevant indicators during examination, conduct closer evaluation of high-risk patients, and achieve early diagnosis and early intervention. The 95% *CI* of each independent risk factor in the multivariate analysis of this study was relatively wide, which was mainly related to the fact that this study was a single-center retrospective study with limited sample size and a low proportion of stage III-IV cases, suggesting that there was a certain sampling variation in the effect of the above risk factors on axillary lymph node metastasis. In the future, it is necessary to expand the sample size and carry out multi-center studies to narrow the confidence interval and improve the stability and extrapolation of the results.

Although this study has clarified the diagnostic advantages of the combined examination, there are still certain objective limitations: first, the sample size is relatively concentrated in a single center, which may have selection bias; second, the stratified analysis of the diagnostic efficacy of breast cancer with different pathological subtypes was not carried out; third, other high-end examination methods such as positron emission tomography were not included for comparison. Future research can further verify the universality of the combined examination by expanding the sample size and carrying out multi-center studies; at the same time, refine the analysis of pathological subtypes to clarify the application value of the combined examination in different types of breast cancer; in addition, artificial intelligence technology can be combined to construct a diagnostic model based on the characteristics of the combined examination, so as to further improve the intelligent and precise level of diagnosis.

In conclusion, the combined examination of ultrasound and contrast-enhanced ultrasound has significant clinical value in the diagnosis of axillary lymph node metastasis in breast cancer. Its diagnostic consistency with pathological results, accuracy, specificity and sensitivity are better than that of single ultrasound and contrast-enhanced ultrasound, and significantly higher than that of traditional MRI and mammography. Meanwhile, tumor diameter $\geq$ 2 cm, maximum cortical thickness of lymph nodes $\geq$ 3 mm, and irregular enhancement pattern in the images of the two examinations are independent risk factors for axillary lymph node metastasis in breast cancer. This combined examination method is convenient to operate, economical and efficient, and can provide a reliable basis for clinical diagnosis and treatment.

Conflict of interest None

Reference

[1] Xu K, Zhang WW, Wang C, et al. Integrative analyses of scRNA-seq and scATAC-seq reveal CXCL14 as a key regulator of lymph node metastasis in breast cancer[J]. Hum Mol Genet, 2021, 30(5): 370-380.

[2] Liu X, Wang MH, Wang Q, et al. Diagnostic value of contrast-enhanced ultrasound for sentinel lymph node metastasis in breast cancer: an updated meta-analysis[J]. Breast Cancer Res Treat, 2023, 202(2): 221-231.

[3] Kim H, Park W, Kim SS, et al. Prognosis of patients with axillary lymph node metastases from occult breast cancer: analysis of multicenter data[J]. Radiat Oncol J, 2021, 39(2): 107-112.

[4] Liu XP, Zha HL, Ping JY, et al. Monitoring of clipped axillary lymph node by ultrasound to predict response of breast cancer to neoadjuvant systemic therapy[J]. J Nanjing Medicial Univ, 2024, 44(6): 845-852. **[In Chinese]**

[5] Ruan Y, Zha GF, Zheng YX, et al. Clinical value of nomogram model based on pathological and ultrasound image features in predicting axillary lymph node metastasis of breast cancer[J]. J Clin Ultrasound Med, 2024, 26(7): 590-595. **[In Chinese]**

[6] Luo J, Feng LT, Zhou Q, et al. The value of contrast-enhanced ultrasound in determining the location of sentinel lymph nodes in breast cancer[J]. Cancer Imaging, 2021, 21(1): 28.

[7] Yao F, Jin F. Surgical management of breast cancer in guidelines of Chinese Society of Clinical Oncology[J]. Chin J Pract Surg, 2018, 38(11): 1281-1284.

[8] Wang H, Yang XW, Chen F, et al. Non-invasive assessment of axillary lymph node metastasis risk in early invasive breast cancer adopting automated breast volume scanning-based radiomics nomogram: a multicenter study[J]. Ultrasound Med Biol, 2023, 49(5): 1202-1211.

[9] Wang YJ, Li YC, Song Y, et al. Comparison of ultrasound and mammography for early diagnosis of breast cancer among Chinese women with suspected breast lesions: a prospective trial[J]. Thorac Cancer, 2022, 13(22): 3145-3151.

[10] Li L, Zhao J, Li FX, et al. Comparison of MRI and ultrasound for evaluation of axillary lymph node status in early breast cancer[J]. Cancer Manag Res, 2024, 16: 1685-1692.

[11] Abel F, Landsmann A, Hejduk P, et al. Detecting abnormal axillary lymph nodes on mammograms using a deep convolutional neural network[J]. Diagnostics, 2022, 12(6): 1347.

[12]Song Y, Liu JJ, Jin CY, et al. Value of contrast-enhanced ultrasound combined with immune-inflammatory markers in predicting axillary lymph node metastasis of breast cancer[J]. Acad Radiol, 2024, 31(9): 3535-3545.

[13] Du HX. Correlation analysis between ultrasonic features of breast cancer and axillary lymph node metastasis[D]. Yangtze University, Jingzhou,2024.**[In Chinese]**

[14] Zhou W, Shi J, Zhou FS, et al. Efficacy of contrast-enhanced ultrasound combined with clinical indicators in predicting axillary lymph node metastasis in breast cancer patients[J]. Chin J Ultrasound Med, 2024, 40(12): 1349-1353. **[In Chinese]**

Submission Received: 2025-12-16/**Revised:** 2026-02-02

· 乳腺癌专题·论著 ·

超声与超声造影在乳腺癌腋窝淋巴结转移诊断中的应用

王鑫[1]，　田丹[1]，　杜敏[2]

1. 北京中医医院内蒙古医院超声科，内蒙古 巴彦淖尔 015000；

2. 北京中医医院内蒙古医院妇科，内蒙古 巴彦淖尔 015000

摘要：目的　分析超声与超声造影联合检查对乳腺癌腋窝淋巴结转移的诊断价值，明确相关独立危险因素。**方法**　回顾性选取2022年1月至2024年12月北京中医医院内蒙古医院收治的102例乳腺癌患者。所有患者均在术前1周内依次完成超声、超声造影、磁共振成像（MRI）、钼靶检查，非同期一次性操作，按临床诊疗规范分时段完成。患者均经病理组织学检查确诊。以术后淋巴结病理结果为金标准，采用Kappa值评估诊断的一致性，受试者工作特征（ROC）曲线评估各项检查的诊断价值，多因素logistic回归筛选独立危险因素（采用逐步回归法控制变量数量）。**结果**　102例患者中，病理确诊淋巴结转移37例（36.27%）。超声与超声造影联合检查的Kappa值为0.936，准确度为0.971，特异度为0.985，灵敏度为0.946。ROC曲线显示，联合检查的曲线下面积为0.965（95%*CI*：0.919~1.000），显著高于单一超声（AUC=0.811，95%*CI*：0.715~0.907）、超声造影（AUC=0.882，95%*CI*：0.802~0.963）、MRI（AUC=0.853，95%*CI*：0.766~0.941）、钼靶检查（AUC=0.803，95%*CI*：0.707~0.900）（$P<0.05$）。多因素logistic回归分析显示，超声与超声造影影像中肿瘤直径≥2 cm、淋巴结最大皮质厚度≥3 mm、增强模式不规则均为乳腺癌腋窝淋巴结转移的独立危险因素（$P<0.05$）。**结论**　超声与超声造影联合检查在乳腺癌腋窝淋巴结转移诊断中具有较高的应用价值，诊断效能优于单一超声、超声造影及传统MRI、钼靶检查，可为临床诊疗提供可靠依据。

关键词：超声；超声造影；乳腺癌；腋窝淋巴结转移；病理学；肿瘤直径；淋巴结皮质厚度

中图分类号：R737.9　**文献标识码：**A　**文章编号：**1674-8182(2026)04-0533-06

Application of ultrasound combined with contrast-enhanced ultrasound in the diagnosis of axillary lymph node metastasis of breast cancer

WANG Xin*, TIAN Dan, DU Min

**Department of Ultrasonography, Inner Mongolia Hospital Beijing Hospital of Traditional Chinese Medicine, Bayannur, Inner Mongolia 015000, China*

Corresponding author: WANG Xin, E-mail: 18547828505@163.com

Abstract: Objective　To analyze the diagnostic value of ultrasound (US) combined with contrast-enhanced ultrasound (CEUS) in axillary lymph node metastasis of breast cancer, and to identify the related independent risk factors. **Methods**　A retrospective selection was made of 102 breast cancer patients admitted to Inner Mongolia Hospital Beijing Hospital of Traditional Chinese Medicine from January 2022 to December 2024. All patients completed US, CEUS, magnetic resonance imaging (MRI), and mammography examinations in sequence within one week before surgery, with non-simultaneous one-time operations, and the examinations were conducted at different time periods in accordance with clinical diagnosis and treatment norms. Patients were diagnosed by histopathological examination. The postoperative lymph node pathological results were used as the gold standard, and Kappa value was used to evaluate the diagnostic consistency of each examination. Receiver operating characteristic (ROC) curve was used to evaluate its

DOI：10.13429/j.cnki.cjcr.2026.04.009

基金项目：内蒙古自治区自然科学基金青年基金项目（2023QN08044）

通信作者：王鑫，E-mail：18547828505@163.com

出版日期：2026-04-20

QR code for English version

diagnostic value, and multivariate logistic regression was used to screen independent risk factors (stepwise regression method was used to control the number of variables). **Results** Among 102 patients, 37 cases (36.27%) were pathologically diagnosed with lymph node metastasis. The Kappa value of US combined with CEUS was 0.936, the accuracy was 0.971, the specificity was 0.985, and the sensitivity was 0.946. ROC curve showed that the area under the curve (AUC) of combined examination was 0.965 (95%*CI*: 0.919-1.000), which was significantly higher than that of single US (AUC=0.811, 95%*CI*: 0.715-0.907), CEUS (AUC=0.882, 95%*CI*: 0.802-0.963), MRI (AUC=0.853, 95%*CI*: 0.766-0.941), and mammography (AUC=0.803, 95%*CI*: 0.707-0.900) ($P<0.05$). Multivariate logistic regression analysis showed that in US and CEUS imaging, tumor diameter ≥2 cm, maximum cortical thickness of lymph nodes ≥3 mm, and irregular enhancement pattern were independent risk factors for axillary lymph node metastasis of breast cancer ($P<0.05$). **Conclusion** The combined examination of US and CEUS has high application value in the diagnosis of axillary lymph node metastasis of breast cancer, and the diagnostic efficacy is better than single US, CEUS, traditional MRI and mammography, which can provide reliable basis for clinical diagnosis and treatment.

Keywords: Ultrasound; Contrast-enhanced ultrasound; Breast cancer; Axillary lymph node metastasis; Pathology; Tumor diameter; Cortical thickness of lymph node

Fund program: Youth Fund Project of Natural Science Foundation of Inner Mongolia Autonomous Region(2023QN08044)

淋巴结转移是乳腺癌常见的转移途径之一,也是影响预后的关键因素。一旦癌细胞通过淋巴管扩散至腋窝淋巴结,临床治疗难度显著增加[1-2]。有研究表明,存在腋窝淋巴结转移的乳腺癌患者5年生存率相较于无转移患者明显降低,且转移淋巴结数量及位置等与患者的复发风险和生存时间密切相关[3]。目前,超声为乳腺癌筛查和诊断的方法之一,能清晰显示乳腺及腋窝淋巴结的形态、结构等,并可观察淋巴结的纵横比、血流信号等特征[4-5],但对微小或不典型转移淋巴结的诊断准确性有限。超声造影可清晰显示淋巴结内部结构和血流分布,对淋巴结转移的诊断敏感度和特异度较高[6],但存在主观性且对技术要求较高。本研究将超声与超声造影联合应用,旨在发挥两者优势,提升乳腺癌腋窝淋巴结转移的诊断准确性,同时明确相关危险因素,为临床提供更优质的诊断方案。

1　资料与方法

1.1　*一般资料*　回顾性选取2022年1月至2024年12月北京中医医院内蒙古医院收治的102例乳腺癌患者,年龄30~81(56.27±10.61)岁;病理类型:浸润性导管癌82例,浸润性小叶癌12例,黏液腺癌5例,其他类型3例。所有患者均签署知情同意书,本研究已获得北京中医医院内蒙古医院医学伦理委员会审批(伦理批号:BIZ20211207)。

1.2　*纳入与排除标准*　(1)纳入标准:①均符合乳腺癌的诊断标准[7],并经病理组织学检查确诊;②年龄≥18岁;③均为女性;④首次单侧发病;⑤术前未接受任何抗肿瘤治疗,可完成完整术前影像学评估。(2)排除标准:①合并其他恶性肿瘤;②对超声造影剂过敏;③存在严重心、肝、肾等重要脏器功能障碍;④存在精神疾病史或认知障碍;⑤已接受新辅助化疗、放疗或内分泌治疗等。

1.3　*仪器设备*　LOGIQ Fortis超声诊断仪[通用电气医疗系统(中国)有限公司],EPIQ7彩色超声诊断系统[飞利浦超声股份有限公司],3.0T磁共振成像系统(西门子医疗系统有限公司),数字化乳腺X线摄影系统(豪洛捷医疗科技有限公司)。

1.4　*方法*　所有影像学资料均由两名经验丰富的医师独立分析,意见不一致时经协商达成一致。所有影像学检查均在术前1周内按超声→超声造影→钼靶→磁共振成像(magnetic resonance imaging, MRI)的顺序分日完成,避免单次检查过多导致患者不适及图像干扰。

1.4.1　超声　采用超声诊断仪,配备频率为4~13 MHz的高频线阵探头。在进行超声检查时,患者需充分暴露胸部,取仰卧位,必要时辅以侧卧位。运用二维超声对双侧乳腺及腋窝进行全面、细致的多切面扫查。仔细观察乳腺的层次结构及肿块位置、大小、形态、边界、内部回声以及后方回声等特征。启动彩色多普勒超声功能,对乳腺肿块及腋窝淋巴结进行血流检测。观察肿块内部及周边的血流信号分布情况,记录血流的丰富程度、血管走行及血流频谱特征。典型病例见图1。

1.4.2　超声造影　在常规超声检查的基础上进行。经肘部静脉快速团注5 mL的超声造影剂(注射用六氟化硫微泡,商品名:SonoVue,厂家:Bracco Suisse SA,批号:F241008Z,以5 mL生理盐水稀释、摇匀),随后立即用10 mL生理盐水快速冲管。在注入造影剂的同时,启动超声诊断仪的造影成像模式,实时动态观

察乳腺肿块及腋窝淋巴结的造影剂灌注情况。观察时间持续3 min，详细记录造影剂开始增强的时间、增强的模式、增强的强度、达峰时间以及廓清的速率等。典型病例见图2。

1.4.3　钼靶　患者取站立位，行双侧乳腺头尾位及内外斜位摄影，必要时加拍侧位片。摄影参数：管电压26~32 kV，管电流60~80 mA，曝光时间0.15~0.35 s，自动曝光控制模式，符合乳腺X线摄影质控标准。

1.4.4　MRI　采用俯卧位，乳腺专用线圈，行横轴位T1WI、T2WI及动态增强扫描。扫描参数：T1WI重复时间500 ms，回波时间10 ms；T2WI重复时间3 000 ms，回波时间80 ms；动态增强扫描采用钆喷酸葡胺作为造影剂，剂量0.1 mmol/kg，经肘部静脉团注后立即扫描，连续扫描5期，每期扫描时间30 s。

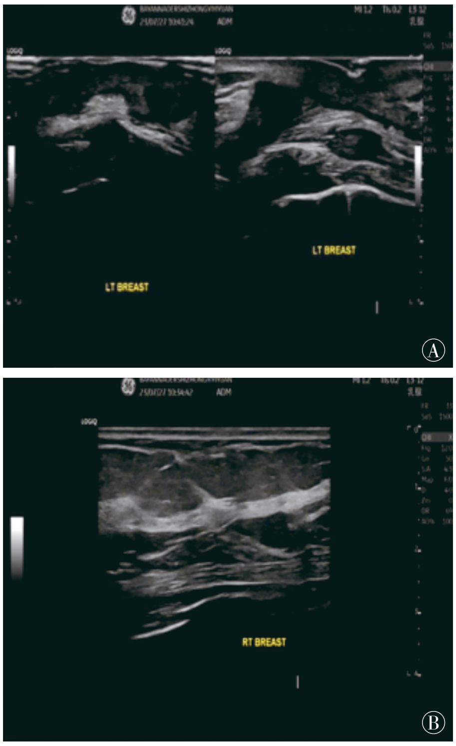

注：A，左侧乳腺切除术后，沿切口走行见不均质低回声，边界清楚，形态不规则，彩色多普勒血流显像（CDFI）显示局部见少量血流信号，内侧切口深方见多个类似低回声，较大者0.78 cm×0.90 cm，边界不清楚，形态不规则，呈浸润形态。B，右侧乳腺腺叶结构清晰，实质回声均匀，未见具体占位。双侧腋下未见明显异常肿大淋巴结。提示左侧乳腺切口瘢痕处及深方多发实性肿物。

图1　典型病例超声检查图

Fig.1　Ultrasound examination images of typical cases

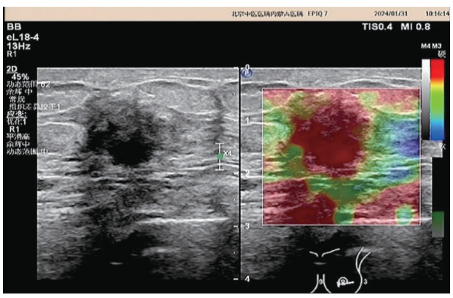

注：乳腺腺叶结构清晰，左乳腺5点钟方向乳头旁见1.58 cm×1.43 cm低回声，形态不规则，边界不清，回声不均，CDFI显示周边及内部可见少量血流信号。提示左乳腺实性结节BI-RADS 4b类。

图2　典型病例超声造影图

Fig.2　Contrast-enhanced ultrasound images of typical cases

1.5　*淋巴结转移的诊断标准*　以术后淋巴结病理检查结果为金标准。超声及超声造影诊断标准：（1）淋巴结肿大，纵横比<2，甚至趋近于1；（2）边界模糊不清，内部回声不均匀；（3）皮质增厚>3 mm；（4）淋巴门被破坏、移位或消失；（5）血流信号丰富，分布不规则，表现为周边型血流或混合型血流；（6）淋巴结内微钙化[8]。根据患者的淋巴结转移情况，将其分为转移组与未转移组。

1.6　*统计学方法*　采用SPSS 26.0软件分析数据。符合正态分布的计量资料用$\bar{x}\pm s$表示，采用t检验。计数资料用例（%）表示，采用χ^2检验或校正χ^2检验。采用Kappa值评估不同检查对乳腺癌腋窝淋巴结转移诊断的一致性。采用受试者工作特征曲线（receiver operating characteristic，ROC）曲线评估联合检查在乳腺癌腋窝淋巴结转移诊断中的价值。多因素logistic回归采用逐步法（$\alpha_{入}$=0.05，$\alpha_{出}$=0.10），控制自变量数量（最终纳入3个变量）。样本量估算基于既往研究的转移率（30%），设定α=0.05、β=0.20，计算最小样本量为92例，本研究102例符合要求。P<0.05为差异有统计学意义。

2　结　果

2.1　*诊断一致性及诊断效能*　102例患者中共有37例（36.27%）出现淋巴结转移。以病理结果为金标准，超声的Kappa值为0.633，准确度为0.833，特异度为0.892，灵敏度为0.730，阳性预测值为0.794，阴性预测值为0.853；超声造影的Kappa值为0.783，准确度为0.902，特异度为0.954，灵敏度为0.811，阳性预测值为0.909，阴性预测值为0.899；MRI的Kappa值为0.719，准确度为0.872，特异度为0.923，灵敏度为0.784，阳性预测值为0.853，阴性预测值为0.882；钼靶的Kappa值为0.614，准确度为0.824，特异度为0.877，灵敏度为0.730，阳性预测值为0.771，阴性预测值为0.851；超声与超声造影联合检查的Kappa值为0.936，准确度为0.971，特异度为0.985，灵敏度为0.946，阳性预测值为0.972，阴性预测值为0.970；由此可见，联合检查的诊断一致性更好，且诊断效能较高。见表1。

2.2　*不同检查的诊断价值*　ROC曲线显示，联合检

查的曲线下面积（area under the curve，AUC）显著高于单一超声、超声造影、MRI、钼靶检查（$P<0.05$）。见图3、表2。

2.3　转移组与未转移组的临床资料对比　转移组年龄、身体质量指数（body mass index，BMI）、绝经、高血压、糖尿病、病理类型、部位等资料与未转移组相比差异均无统计学意义（$P>0.05$）；而TNM分期比较差异有统计学意义（$P<0.05$）。见表3。

2.4　转移组与未转移组的影像学特征对比　转移组的脉管侵犯、内部回声不均匀、后方回声衰减、形状不规则、钙化、边缘毛刺征、纵横比、血流分级、淋巴结最大纵径、增强程度、结构扭曲、增强后边界清晰、增强后范围扩大、增强后灌注缺损、增强后边缘出现放射汇聚等资料与未转移组相比，差异无统计学意义（$P>0.05$）；而两组肿瘤直径、淋巴结最大皮质厚度、增强模式不规则相比，差异有统计学意义（$P<0.05$）。见表4。

表1　淋巴结转移诊断一致性　（n=102，例）

Tab.1　Consistency in lymph node metastasis diagnosis （n=102，case）

项目		病理结果		合计
		阳性（n=37）	阴性（n=65）	
超声	阳性	27	7	34
	阴性	10	58	68
超声造影	阳性	30	3	33
	阴性	7	62	69
MRI	阳性	29	5	34
	阴性	8	60	68
钼靶	阳性	27	8	35
	阴性	10	57	67
超声与超声造影联合检查	阳性	35	1	36
	阴性	2	64	66

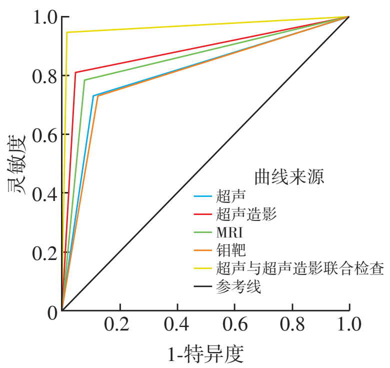

图3　不同检查诊断乳腺癌腋窝淋巴结转移的ROC曲线

Fig.3　ROC curves of different examinations for the diagnosis of axillary lymph node metastasis in breast cancer

表2　不同检查对乳腺癌腋窝淋巴结转移的诊断价值

Tab.2　Diagnostic value of different examinations for axillary lymph node metastasis in breast cancer

变量	AUC	*SE*	*P*值	95%*CI*
超声	0.811	0.049	<0.001	0.715~0.907
超声造影	0.882	0.041	<0.001	0.802~0.963
MRI	0.853	0.044	<0.001	0.766~0.941
钼靶	0.803	0.049	<0.001	0.707~0.900
超声与超声造影联合检查	0.965	0.023	<0.001	0.919~1.000

表3　转移组与未转移组的临床资料对比

Tab.3　Comparison of clinical data between metastatic group and non-metastatic group

项目	转移组（n=37）	未转移组（n=65）	t/χ^2值	*P*值
年龄（岁，$\bar{x}\pm s$）	55.59±10.81	56.66±10.55	0.488	0.626
BMI（kg/m², $\bar{x}\pm s$）	22.16±1.42	22.51±1.53	1.140	0.257
绝经［例（%）］	14（37.84）	35（53.85）	2.421	0.120
高血压［例（%）］	13（35.14）	24（36.92）	0.033	0.857
糖尿病［例（%）］	10（27.03）	15（23.08）	0.199	0.656
TNM分期［例（%）］				
Ⅰ~Ⅱ期	15（40.54）	60（92.31）	32.464	<0.001
Ⅲ~Ⅳ期	22（59.46）	5（7.69）		
病理类型［例（%）］				
浸润性导管癌	30（81.08）	52（80.00）	0.090	0.993
浸润性小叶癌	4（10.81）	8（12.31）		
黏液腺癌	2（5.41）	3（4.62）		
其他类型	1（2.70）	2（3.07）		
侧别［例（%）］				
左侧	16（43.24）	24（36.92）	0.395	0.530
右侧	21（56.76）	41（63.08）		

表4　转移组与未转移组的影像学特征对比　［例（%）］

Tab.4　Comparison of imaging features between the metastatic group and the non-metastatic group　［case（%）］

项目	转移组（n=37）	未转移组（n=65）	χ^2值	*P*值
脉管侵犯	22（59.46）	36（55.38）	0.160	0.690
内部回声不均匀	25（67.57）	32（49.23）	3.216	0.073
后方回声衰减	11（29.73）	16（24.62）	0.317	0.573
形状不规则	26（70.27）	42（64.62）	0.339	0.560
钙化	15（40.54）	22（33.85）	0.457	0.499
边缘毛刺征	17（45.95）	40（61.54）	2.325	0.127
肿瘤直径				
<2 cm	9（24.32）	52（80.00）	30.404	<0.001
≥2 cm	28（75.68）	13（20.00）		
纵横比				
<1	15（40.54）	34（52.31）	1.308	0.253
≥1	22（59.46）	31（47.69）		
血流分级				
Ⅰ~Ⅱ级	14（37.84）	37（56.92）	3.435	0.064
Ⅲ级	23（62.16）	28（43.08）		
淋巴结最大纵径				
<1 cm	26（70.27）	55（84.62）	2.968	0.085
≥1 cm	11（29.73）	10（15.38）		
淋巴结最大皮质厚度				
<3 mm	8（21.62）	50（76.92）	29.397	<0.001
≥3 mm	29（78.38）	15（23.08）		
增强程度				
低增强/等增强	6（16.22）	10（15.38）	0.012	0.912
高增强	31（83.78）	55（84.62）		
结构扭曲	7（18.92）	4（6.15）	2.777	0.096
增强模式不规则	30（81.08）	26（40.00）	16.071	<0.001
增强后边界清晰	9（24.32）	19（29.32）	0.285	0.593
增强后范围扩大	30（81.08）	42（64.62）	3.079	0.079
增强后灌注缺损	12（32.43）	17（26.15）	0.457	0.499
增强后边缘出现放射汇聚	11（29.73）	15（23.08）	0.549	0.459

2.5 超声和超声造影影像中乳腺癌腋窝淋巴结转移的多因素logistic回归分析 多因素logistic回归分析果显示，肿瘤直径≥2 cm、淋巴结最大皮质厚度≥3 mm、增强模式不规则均为乳腺癌腋窝淋巴结转移的独立危险因素（$P<0.05$）。见表5。

表5 乳腺癌腋窝淋巴结转移的多因素logistic回归分析
Tab.5 Multivariate logistic regression analysis of axillary lymph node metastasis in breast cancer

指标	β	SE	Wald χ^2	OR值	95%CI	P值
肿瘤直径≥2 cm	1.286	0.626	4.222	3.619	1.061~12.343	0.040
淋巴结最大皮质厚度≥3 mm	1.277	0.629	4.120	3.587	1.045~12.314	0.042
增强模式不规则	1.217	0.609	3.993	3.377	1.024~11.139	0.046

3 讨 论

本研究核心聚焦超声与超声造影联合检查对乳腺癌腋窝淋巴结转移的诊断价值，并通过与MRI、钼靶的直接对比，明确其临床应用优势。从诊断一致性来看，联合检查与病理结果一致性的Kappa值高达0.936，远高于单一超声（0.633）、超声造影（0.783）、MRI（0.719）及钼靶（0.614），表明联合检查与病理金标准的吻合度极高，诊断结果更可靠。在诊断效能方面，联合检查的准确度（0.971）、特异度（0.985）、灵敏度（0.946）均显著优于单一检查方法。这一优势的本质是两种技术的互补协同：超声可清晰呈现淋巴结的形态学特征（如大小、边界、皮质厚度等），为初步判断提供结构基础[9]；超声造影则能精准展示血流灌注模式，转移性淋巴结常表现出的不规则增强、灌注缺损等特征，可有效区分形态相似的反应性增生淋巴结。而MRI虽软组织分辨率高，但受呼吸运动干扰较大，对微小转移灶的检出率有限，且检查成本高、耗时久，不利于基层推广[10]；钼靶对钙化灶敏感，但对致密型乳腺组织穿透力不足，对腋窝淋巴结的显示效果较差[11]，导致其灵敏度仅为0.730，低于联合检查。ROC曲线分析进一步证实，联合检查的AUC（0.965）显著高于MRI（0.853）和钼靶（0.803），说明其诊断准确性更高，能更有效地鉴别腋窝淋巴结是否转移，为临床治疗方案的制定提供关键依据。

本研究通过多因素logistic回归分析，明确超声和超声造影影像中肿瘤直径≥2 cm、淋巴结最大皮质厚度≥3 mm、增强模式不规则为乳腺癌腋窝淋巴结转移的独立危险因素。肿瘤直径越大，癌细胞突破基底膜、侵入淋巴管的概率越高，发生淋巴结转移的风险也随之增加[12]；淋巴结最大皮质厚度≥3 mm反映了淋巴结结构的异常增生，是转移灶侵犯的直接表现[13]；增强模式不规则则提示淋巴结内部血流灌注紊乱，与转移性病灶的侵袭性生物学行为密切相关[14]。这些危险因素的明确，有助于临床医师在检查中重点关注相关指标，对高风险患者进行更密切的评估，实现早诊断、早干预。本研究多因素分析中各独立危险因素的95%CI相对较宽，主要与本研究为单中心回顾性研究、样本量有限、Ⅲ~Ⅳ期病例占比较低有关，提示上述危险因素对腋窝淋巴结转移的影响效应存在一定的抽样变异，未来需扩大样本量、开展多中心研究以缩小置信区间、提升结果的稳定性与外推性。

本研究虽明确了联合检查的诊断优势，但仍存在一定的客观局限性：一是样本量相对集中于单中心，可能存在选择偏倚；二是未对不同病理亚型乳腺癌的诊断效能进行分层分析；三是未纳入正电子发射断层扫描等其他高端检查方法进行对比。未来研究可通过扩大样本量、开展多中心研究，进一步验证联合检查的普适性；同时细化病理亚型分析，明确联合检查在不同类型乳腺癌中的应用价值；此外，可结合人工智能技术，构建基于联合检查特征的诊断模型，进一步提升诊断的智能化与精准化水平。

综上所述，超声与超声造影联合检查在乳腺癌腋窝淋巴结转移诊断中具有显著的临床价值，其与病理结果的诊断一致性、准确度、特异度及灵敏度均优于单一超声、超声造影，且明显高于传统MRI及钼靶检查。同时，二者影像中肿瘤直径≥2 cm、淋巴结最大皮质厚度≥3 mm、增强模式不规则是乳腺癌腋窝淋巴结转移的独立危险因素。该联合检查方法操作便捷、经济高效，可为临床诊疗提供可靠依据。

利益冲突 无

参考文献

[1] Xu K, Zhang WW, Wang C, et al. Integrative analyses of scRNA-seq and scATAC-seq reveal CXCL14 as a key regulator of lymph node metastasis in breast cancer[J]. Hum Mol Genet, 2021, 30(5): 370-380.

[2] Liu X, Wang MH, Wang Q, et al. Diagnostic value of contrast-enhanced ultrasound for sentinel lymph node metastasis in breast cancer: an updated meta-analysis[J]. Breast Cancer Res Treat, 2023, 202(2): 221-231.

[3] Kim H, Park W, Kim SS, et al. Prognosis of patients with axillary lymph node metastases from occult breast cancer: analysis of multicenter data[J]. Radiat Oncol J, 2021, 39(2): 107-112.

[4] 刘心培，查海玲，平洁怡，等. 超声监测定位腋窝淋巴结对乳腺癌患者新辅助治疗疗效的预测研究[J]. 南京医科大学学报（自然科学版），2024, 44(6): 845-852.

（下转第542页）

危险因素。提示在临床病理特征相似的患者中，TRPS1高表达者其疾病复发或转移的风险是低表达者的2.3倍以上。其机制可能在于TRPS1核心促癌功能的持续性。TRPS1通过促进增殖、侵袭、EMT，可能影响肿瘤干细胞特性或治疗抵抗，最终导致了更高的复发转移风险[16-17]。本研究为TRPS1的预后价值提供了来自中国人群的临床证据，与Ai等[8]报道的TRPS1高表达与较短的总生存期和无病生存期相关的结论相互印证。因此，在临床中，对TRPS1高表达乳腺癌，尤其是早期、无淋巴结转移者，应加强随访，积极辅助治疗以改善患者的生存。

3.4　*研究的局限性与展望*　本研究存在以下局限性：首先，本研究为单中心回顾性队列研究，样本量小，存在选择偏倚风险；其次，随访时长仅为3年，未能对TRPS1在长期生存方面的影响进行评估；最后，仅在蛋白表达层面开展了相关性分析，尚未深入探究其调控乳腺癌进展的具体分子作用机制。未来可开展多中心大样本前瞻性研究以验证其预后价值；延长随访时间以评估其对长期生存的意义。

综上所述，本研究证实了新型标志物TRPS1在IBC-NST组织中高表达，其表达水平与组织学分级、TNM分期、淋巴结转移及TNBC亚型等不良临床病理特征密切相关，且TRPS1可用来预测乳腺癌预后。

利益冲突　无

参考文献

[1]　吴均，任晓秋，杨君，等. 浸润性乳腺癌合并的导管内癌成分与腋窝淋巴结转移的相关性研究[J]. 临床肿瘤学杂志，2021，26(10)：914-919.
[2]　张伟，刘霞，何雷，等. 浸润性乳腺癌中miR-608和MIF的表达及临床意义[J]. 临床与实验病理学杂志，2022，38(1)：1-8.
[3]　胡月，王稼良，胡飞翔，等. 三阴性乳腺癌免疫微环境与免疫治疗的研究进展[J]. 中国临床研究，2024，37(10)：1477-1482.
[4]　刘丽敏，孙晶晶，钱佳骏，等. TRPS1在唾液腺肿瘤中的表达及诊断价值[J]. 临床口腔医学杂志，2024，40(7)：393-397.
[5]　Recio SG，Hinoue T，Wheeler GL，et al. Abstract LB176：multiplatform analysis of matched primary and metastatic breast tumors from the AURORA US Network identifies microenvironment features as drivers of metastasis[J]. Cancer Res，2022，82(12_Supplement)：LB176.
[6]　Lennartz M，Löhr N，Höflmayer D，et al. TRPS1 is a highly sensitive marker for breast cancer：a tissue microarray study evaluating more than 19，000 tumors from 152 different tumor entities[J]. Am J Surg Pathol，2024，48(6)：637-651.
[7]　刘玥，许颂华，连秀丽，等. 转录因子TRPS1通过H3K27me3调控小鼠合子型基因激活[J]. 解剖学杂志，2021，44(S1)：177.
[8]　Ai D，Yao J，Yang F，et al. TRPS1：a highly sensitive and specific marker for breast carcinoma，especially for triple-negative breast cancer[J]. Mod Pathol，2021，34(4)：710-719.
[9]　李菲，李静，杜丽，等. TRPS1、GATA3在乳腺癌中的表达及其临床意义[J]. 妇儿健康导刊，2023，2(10)：14-16，封4.
[10]　徐静纯，戴桂红，王璐，等. 毛发鼻指(趾)综合征-1基因在乳腺癌中的研究进展[J]. 实用临床医药杂志，2025，29(6)：143.
[11]　樊艳，栗粟，田天，等. miR-511-5p/FEM1C轴通过激活自噬对乳腺癌细胞增殖和侵袭的影响[J]. 临床肿瘤学杂志，2024，29(2)：105-113.
[12]　杨依琳，刘超，毛伟征. 微RNA在乳腺癌发病机制及预后预测中的作用研究进展[J]. 医学综述，2023，29(12)：2367-2371.
[13]　Cai JQ，Zhang WL，Lu YL，et al. Single-cell exome sequencing reveals polyclonal seeding and TRPS1 mutations in colon cancer metastasis[J]. Signal Transduct Target Ther，2024，9(1)：247.
[14]　肖诗维，金苏，岳君秋，等. TRPS1蛋白在乳腺癌肺转移灶中的诊断应用价值[J]. 临床与实验病理学杂志，2024，40(9)：967.
[15]　赵萌，何建坤，刘月平. 乳腺转移性无色素性上皮样黑色素瘤6例临床病理及分子遗传学特征[J]. 临床与实验病理学杂志，2022，38(11)：1309-1312.
[16]　Liu JF，Wu BE，Wan SH，et al. Upregulation of TRPS1 promotes proliferation，migration，and invasion in ovarian clear cell carcinoma and correlates with poor patient prognosis[J]. J Ovarian Res，2025，18(1)：73.
[17]　茅芯慧，王珍，朱成斌. LncRNA ZEB2-AS1通过miR-27b/FZD7轴调控乳腺癌细胞增殖、侵袭和上皮间质转化的研究[J]. 中国性科学，2022，31(2)：49-55.

收稿日期：2025-12-12　**修回日期**：2026-02-10　**编辑**：王宇

（上接第537页）

[5]　阮彦，查国芬，郑雨欣，等. 基于病理和超声图像特征的列线图模型预测乳腺癌腋窝淋巴结转移的临床价值[J]. 临床超声医学杂志，2024，26(7)：590-595.
[6]　Luo J，Feng LT，Zhou Q，et al. The value of contrast-enhanced ultrasound in determining the location of sentinel lymph nodes in breast cancer[J]. Cancer Imaging，2021，21(1)：28.
[7]　姚凡，金锋.《中国临床肿瘤学会乳腺癌诊疗指南2018.V1》外科问题解读[J]. 中国实用外科杂志，2018，38(11)：1281-1284.
[8]　Wang H，Yang XW，Chen F，et al. Non-invasive assessment of axillary lymph node metastasis risk in early invasive breast cancer adopting automated breast volume scanning-based radiomics nomogram：a multicenter study[J]. Ultrasound Med Biol，2023，49(5)：1202-1211.
[9]　Wang YJ，Li YC，Song Y，et al. Comparison of ultrasound and mammography for early diagnosis of breast cancer among Chinese women with suspected breast lesions：a prospective trial[J]. Thorac Cancer，2022，13(22)：3145-3151.
[10]　Li L，Zhao J，Li FX，et al. Comparison of MRI and ultrasound for evaluation of axillary lymph node status in early breast cancer[J]. Cancer Manag Res，2024，16：1685-1692.
[11]　Abel F，Landsmann A，Hejduk P，et al. Detecting abnormal axillary lymph nodes on mammograms using a deep convolutional neural network[J]. Diagnostics，2022，12(6)：1347.
[12]　Song Y，Liu JJ，Jin CY，et al. Value of contrast-enhanced ultrasound combined with immune-inflammatory markers in predicting axillary lymph node metastasis of breast cancer[J]. Acad Radiol，2024，31(9)：3535-3545.
[13]　杜荷霞. 乳腺癌超声特征与腋窝淋巴结转移的相关性分析[D]. 荆州：长江大学，2024.
[14]　周婉，施静，周锋盛，等. 超声造影联合临床指标预测乳腺癌患者腋窝淋巴结转移的效能[J]. 中国超声医学杂志，2024，40(12)：1349-1353.

收稿日期：2025-12-16　**修回日期**：2026-02-02　**编辑**：王宇